Available online at www.sciencedirect.com
ScienceDirect
Trans. Nonferrous Met. Soc. China 25(2015) 3348−3353
Transactions of Nonferrous Metals Society of China
www.tnmsc.cn

Effect of element fitting on composition optimization of Al−Cu−Ti amorphous alloy by mechanical alloying

Zhen TAN[1], Yun-fei XUE[1,2], Xing-wang CHENG[1,2], Long ZHANG[3], Wei-wei CHEN[1,2], Lu WANG[1,2], Hai-feng ZHANG[3], Hua-meng FU[3]

1. School of Materials Science and Engineering, Beijing Institute of Technology, Beijing 100081, China;
2. National Key Laboratory of Science and Technology on Materials under Shock and Impact, Beijing 100081, China;
3. Shenyang National Laboratory for Materials Science, Institute of Metal Research, Chinese Academy of Sciences, Shenyang 110016, China

Received 25 November 2014; accepted 7 May 2015

Abstract: In order to minimize the crystal phase in Al−Cu−Ti amorphous powder, $Al_{65}Cu_{35-x}Ti_x$ amorphous powders were optimized via ball milling through adjusting the amount of Cu and Ti elements and the ball milling time. The results show that increasing the mole fraction of Ti can decrease the amount of $AlCu_2Ti$, Cu_9Al_4, and Al_2Cu intermetallics formed during the process of ball milling; and prolonging the ball milling time can reduce the element crystalline phase to almost none. The optimal composition is determined to be $Al_{65}Cu_{16.5}Ti_{18.5}$. TiH_2 forms in all selected $Al_{65}Cu_{35-x}Ti_x$ amorphous powders during the process of optimization. H atom is decomposed from toluene and reacts with Ti during ball milling, leading to the formation of TiH_2. The volume fraction of TiH_2 in $Al_{65}Cu_{16.5}Ti_{18.5}$ amorphous powder is measured to be 4.30%.

Key words: Al-based amorphous alloy; process optimization; wet milling; TiH_2

1 Introduction

In recent years, Al-based amorphous alloys have attracted considerable attention due to high strength and low density. Currently, rapid quenching (RQ) and mechanical alloying (MA) are the main methods of synthesizing Al-based amorphous alloys [1,2]. However, some kinds of Al-based amorphous alloys with promising excellent mechanical properties but low glass forming ability (GFA) cannot be prepared through RQ. MA provides possibility for preparing these amorphous alloys due to that MA possesses distinct mechanism of amorphization [3−5]. Thus, much attention has been paid to the synthesis of Al-based amorphous alloy by mechanical alloying [6−8].

Although ball milling element powders within a wide range of mole fraction can achieve amorphous or amorphous/nanocrystalline alloys, there exists an optimum mole fraction, which can reduce the residual crystal phase to the minimum level [9]. The present work attempted to obtain the optimal composition of Al−Cu−Ti alloy by adjusting the mole fractions of Cu and Ti. The structural evolution of the powders during optimizing process was investigated in detail.

When several ductile powders are ball-milled, the effect of cold welding may be stronger than that of fracturing, resulting in the aggregation of powders. The wet mechanical alloying seems to be an appropriate technique to produce alloyed powders with reduced average particle size of ductile elements [10]. Process control agent (PCA) is added during wet milling. The process control agents are usually organic substances, such as stearic acid cyclohexane and methanol [11,12]. However, the presence of PCA is also the source of contamination during milling, such as oxygen, carbon and hydrogen. [11−13]. During the process of optimization, TiH_2 is formed as a new compound in the present work. In general, TiH_2 may be obtained by the reaction between element Ti and hydrogen atmosphere. However, there is no hydrogen atmosphere. Thus, the formation and content of TiH_2 were investigated in

Foundation item: Projects (51271036, 51471035, 51101018) supported by the National Natural Science Foundation of China; Project supported by the Program of "One Hundred Talented People" of the Chinese Academy of Sciences
Corresponding author: Lu WANG; Tel: +86-10-68912709 ext. 107; Fax: +86-10-68911144 ext. 869; E-mail: wanglu@bit.edu.cn
DOI: 10.1016/S1003-6326(15)63969-3

detail, which may broaden the horizon of preparing TiH_2 without hydrogen atmosphere.

2 Experimental

The element powders of Al (~50 μm, purity ≥99.5%), Cu (~50 μm, purity ≥ 99.5%) and Ti (~50 μm, purity ≥ 99.5%) were ball-milled to produce $Al_{65}Cu_{35-x}Ti_x$ powders (x=13.5, 15.0, 16.5, 17.5 and 18.5). A high energy ball mill (SPEX 8000D) was employed to mechanically alloying the as-mixed powders under argon atmosphere. Toluene was added as the process control agent (PCA) to prevent the agglomeration of particles during ball milling.

The phase identification was characterized by X-ray diffraction (XRD) using a Philips diffractometer with Cu K_α radiation. The X-ray diffraction spectroscopy was analyzed by Lorentzian multi-peak fitting to obtain the intensity, location, and full width at half maximum (FWHM) of every peak. Scherrer formula was used to estimate the crystal grain size:

$$D=0.89\lambda/(\beta\cos\theta) \quad (1)$$

where D is the average grain diameter, λ is the wavelength of X-ray, β and θ stand for the full width at half maximum and the location, respectively. The morphology of the powders was examined by scanning electron microscopy (SEM, HITACHI S4800). The microstructure of the powders was verified by high-resolution transmission electron microscopy (HRTEM) using a TECNAI F30 with an accelerating voltage of 300 kV. The thermal analyses were examined by differential scanning calorimetry (DSC) and thermo-gravimetric (TG) using METTLER TOLED TGA/DSC at a fixed heating rate of 10 K/min in a high-purity flowing argon atmosphere.

3 Results

Figure 1 shows the XRD patterns of $Al_{65}Cu_{35-x}Ti_x$ (x=13.5, 15.0, 16.5, 17.5 and 18.5) powders after ball milling for 20 h. The designed composition alloys exhibit a mixture of amorphous phase and several crystal phases. The difference of atomic composition induces different contents and crystal phases. $AlCu_2Ti$ (220), Cu_9Al_4 (330), and Al_2Cu (220) peaks appear on the XRD patterns of $Al_{65}Cu_{35-x}Ti_x$ (x=13.5, 15.0, 16.5 and 17.5), while Al(111), Ti(101) and Al_2Cu (220) peaks appears on $Al_{65}Cu_{16.5}Ti_{18.5}$. The intensities of $AlCu_2Ti$ (220), Cu_9Al_4 (330) and Al_2Cu (220) peaks decrease gradually with increasing x from 13.5 to 18.5, as shown in Fig. 1.

Figure 2 shows the XRD patterns of $Al_{65}Cu_{35-x}Ti_x$ powders after ball milling for 30 h. Compared with those in Fig. 1, the most dramatic change occurs in $Al_{65}Cu_{16.5}Ti_{18.5}$ powder. After ball milling for 30 h, the peaks of elements Al and Ti disappear completely. Prolonging the ball milling time induces no significant phase transformation except for further broadening the existing peaks of $Al_{65}Cu_{35-x}Ti_x$ (x=13.5, 15.0, 16.5 and 17.5) powders due to the grain refinement. The grain size decreases from (14±0.5) to (12±0.5) nm for Al_2Cu, (10±0.5) to (8±0.5) nm for Cu_9Al_4 and (9±0.5) to (8±0.5) nm for $AlCu_2Ti$ with increasing the ball milling time from 20 to 30 h.

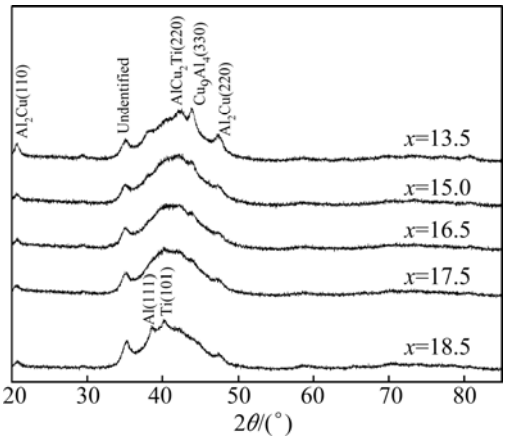

Fig. 1 XRD patterns of $Al_{65}Cu_{35-x}Ti_x$ alloys after ball milling for 20 h

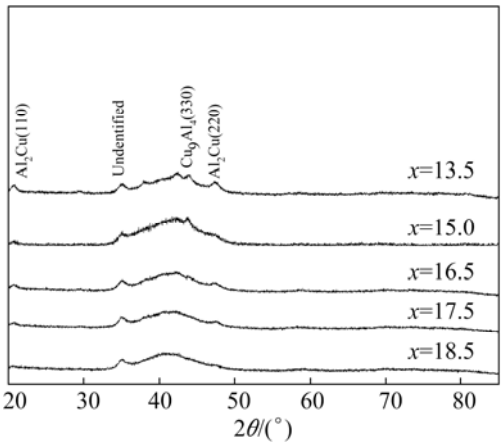

Fig. 2 XRD patterns of $Al_{65}Cu_{35-x}Ti_x$ alloys after ball milling for 30 h

Figures 3(a) and (b) show the microstructures of $Al_{65}Cu_{16.5}Ti_{18.5}$ amorphous powder after ball milling for 20 and 30 h, respectively. Both of the $Al_{65}Cu_{16.5}Ti_{18.5}$ powders exhibit similar size and shape, and the size of all the irregular particles is less than 10 μm.

The unidentified phase appearing at 2θ = 36° on the XRD patterns of $Al_{65}Cu_{35-x}Ti_x$ powders in Figs. 1 and 2 is identified as TiH_2 (111) (PDF card No. 09−0371) by Jade 6.0 software. Figure 4 shows the HRTEM image of $Al_{65}Cu_{16.5}Ti_{18.5}$ amorphous powder after ball milling for 30 h, exhibiting crystal phases in the amorphous matrix.

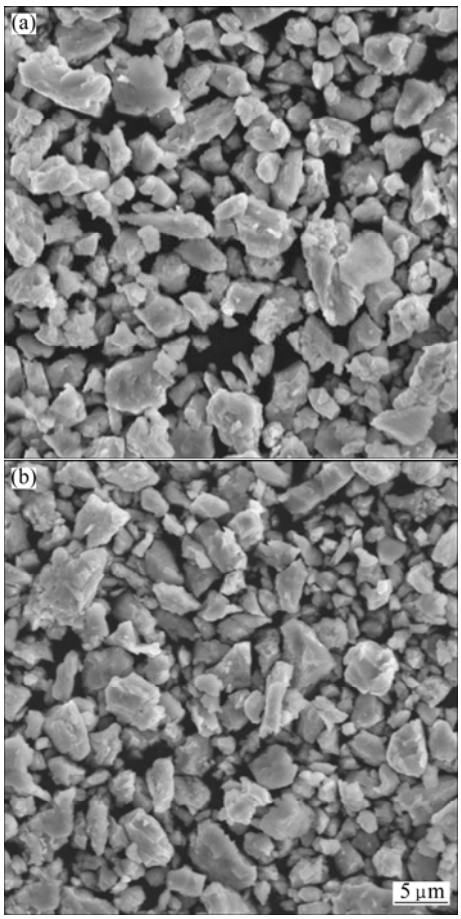

Fig. 3 Microstructures of $Al_{65}Cu_{16.5}Ti_{18.5}$ powders after ball milling for 20 h (a) and 30 h (b)

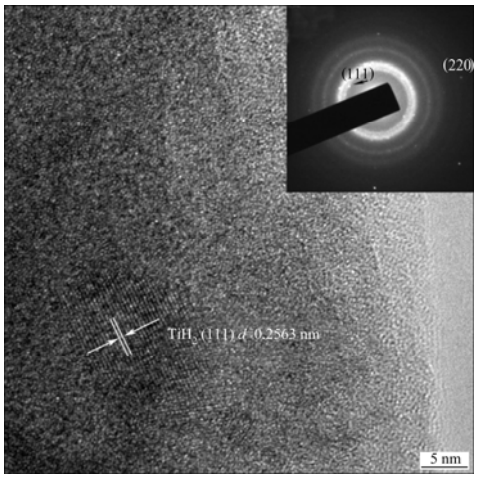

Fig. 4 HRTEM and corresponding SAED images of $Al_{65}Cu_{16.5}Ti_{18.5}$ alloy after ball milling for 30 h

The value of interplanar spacing measured from the HRTEM image is 0.2563 nm, which equals the PDF data of TiH_2. The lattice constant calculated from the SAED patterns also equals the PDF data of TiH_2. Thus, the crystal phase appearing in the HRTEM image of $Al_{65}Cu_{16.5}Ti_{18.5}$ amorphous powder is identified to be TiH_2 (111).

In order to investigate the formation of TiH_2, Ti element powder was ball-milled for 20 h with toluene as the PCA. For comparison, Al powder was also ball-milled. Figure 5 shows the XRD patterns of ball-milled Ti and Al powders with toluene for 20 h. However, no TiH_2 was found in the XRD patterns.

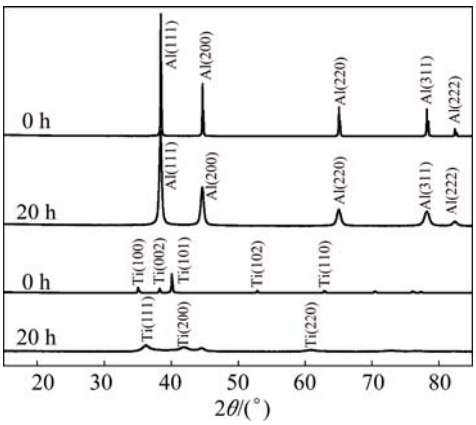

Fig. 5 XRD patterns of Al and Ti after ball milling for 0 h and 20 h

Given the catalysis of Al element during the formation of TiH_2, $Al_{50}Ti_{50}$ mixed powder was ball-milled for 20 h with toluene as the PCA. Figure 6 shows the XRD patterns of $Al_{50}Ti_{50}$ powder after ball milling for 20 h with toluene as the PCA. TiH_2 peak as well as Al_3Ti peaks appear in the XRD patterns of $Al_{50}Ti_{50}$ powder after ball milling for 20 h with toluene.

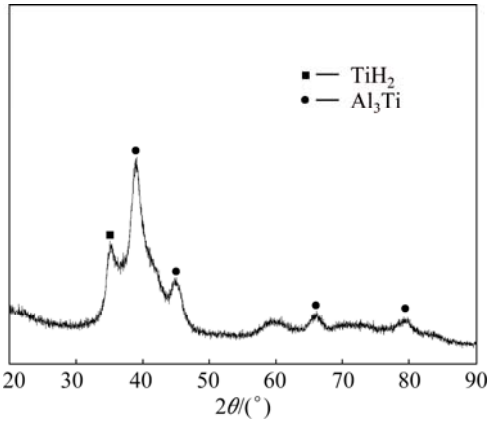

Fig. 6 XRD pattern of $Al_{50}Ti_{50}$ powders after ball milling for 20 h

Since TiH_2 in the ball-milled powder is thermal metastable, the content of TiH_2 can be obtained based on the dehydrogenation of TiH_2. Figure 7 shows the TG and DTG plots obtained by heating the ball-milled $Al_{65}Cu_{16.5}Ti_{18.5}$ amorphous powder. The mass loss occurs from 300 to 825 K, as shown in the TG plot. The corresponding DTG plot shows that the mass loss ratio against temperature is different in the two major stages ranging from 300 to 673 K and 675 to 823 K. There may

be still some residual toluene in the amorphous powder although the powder was annealed at low temperature. Thus, the mass loss at the stage from 300 to 673 K is mainly attributed to the evaporation of toluene. The decomposition of TiH_2 mainly occurs from 675 to 823 K. As a consequence, the mass loss caused by TiH_2 decomposition is about 0.17%. The decomposition of TiH_2 is described as

$$TiH_2\ (s) \longrightarrow Ti\ (s) + H_2\ (g) \quad (2)$$

The mass loss is induced by hydrogen escape during the decomposition of TiH_2. As a consequence, the mass fraction of TiH_2 can be calculated to be 4.25% based on the mass conservation. The volume fraction can also be calculated to be 4.30% by substituting into the density of TiH_2 (3.76 g/cm^3) and $Al_{65}Cu_{16.5}Ti_{18.5}$ amorphous powder (3.81 g/cm^3).

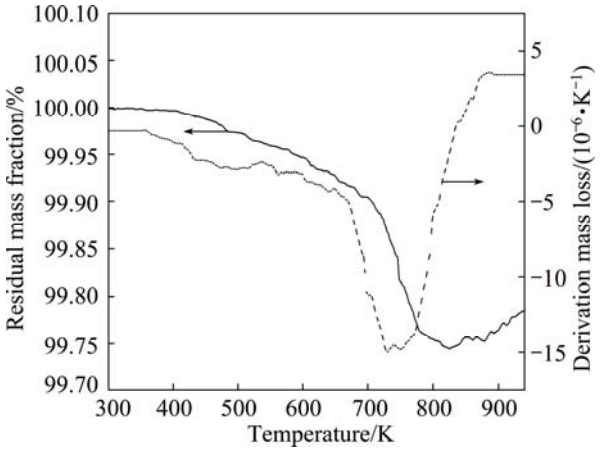

Fig. 7 TG and DTG plots of $Al_{65}Cu_{16.5}Ti_{18.5}$ amorphous powders after ball milling for 30 h

4 Discussion

According to the XRD patterns of $Al_{65}Cu_{35-x}Ti_x$ (x=13.5, 15.0, 16.5, 17.5 and 18.5) powders after ball milling for 20 h, the contents of Cu_9Al_4 and $AlCu_2Ti$ phases decrease with increasing the Ti content from 13.5 to 18.5, indicating that Ti has significant effect on the formation of amorphous phase, which induces the phase transformation from intermetallics to amorphous phase. The completely dissolved time of element Ti increases with increasing the mole fraction of Ti in $Al_{65}Cu_{35-x}Ti_x$ powder, while Al keeps element state instead of forming compounds due to the lack of Cu. As a consequence, there are still elements Al and Ti peaks in the XRD patterns of $Al_{65}Cu_{16.5}Ti_{18.5}$ after ball milling for 20 h, as shown in Fig. 1.

The prolongation of ball milling time promotes the diffusion of Al and Ti elements, resulting in the formation of amorphous phase. Because the processes of cold-welding and fragmentation reach the dynamic balance state after ball milling for 20 h, the average size of powders changes little during prolonging the ball milling time, as shown in Fig. 3.

Although energy is continuously input to the powders by prolonging the ball milling time, there is no phase transformation in $Al_{65}Cu_{35-x}Ti_x$ (x=13.5, 15.0, 16.5 and 17.5) powders, as shown in Figs. 1 and 2. As a dynamic process, ball milling often exhibits steady-state microstructure under balance condition, thus sufficiently large energy can be stored in the steady-state microstructure [14,15]. The steady-state microstructure is a mixture of amorphous phase and intermetallic compounds.

The phase transformation occurs in $Al_{65}Cu_{16.5}Ti_{18.5}$ powder with increasing the ball milling time. It is remarkable to note that intermetallic compounds are much more stable than element phases, because the diffusion of elements in compounds is more difficult than that in element phases during ball milling. $Al_{65}Cu_{16.5}Ti_{18.5}$ powder shows mixed phases of amorphous phase and unidentified crystalline after completing the phase transformation, as shown in Fig. 2. The unidentified crystalline phase is considered not to be element crystalline phase.

Although there is no TiH_2 in the ball-milled Ti and Al powders with toluene for 20 h, a remarkable structure transformation of Ti is found (Fig. 6). Ball milling for 20 h not only leads to the increase of peak width and the decrease of peak intensity, but also makes Ti peaks shift towards higher 2θ, indicating the formation of FCC Ti. However, there is no FCC Ti in the initial Ti powder and Ti does not possess any equilibrium FCC structure at room or elevated temperatures [16]. The transformation from HCP Ti to FCC Ti occurs during ball milling, and the same phenomenon was also observed in some researches [17,18]. The HCP−FCC polymorphic change in Ti is attributed to the combined effect of nanocrystallisation and crystal defects introduced by ball milling.

Ti cannot react with toluene directly, while local high temperature induced by high-energy ball milling with the catalysis effect of Al atom may lead to the decomposition of toluene, resulting in the formation of H atoms. Subsequently, H reacts with Ti quickly, resulting in the formation of TiH_2 phase. TiH_2 does not appear during the first 6 h of ball milling, because FCC Ti is believed to absorb H atom more easily than HCP Ti for more slip systems in FCC Ti [19], and there is nearly no FCC Ti in the initial stage of ball milling with the ball milling time less than 20 h. As a consequence, the formation of TiH_2 results from the joint effects of transformation of HCP−FCC Ti and formation of H atoms decomposed from toluene. Free H atoms diffuse into FCC Ti after FCC Ti forms to form TiH_2. Only

small amount of free H atoms can be decomposed from toluene, thus the amount of TiH_2 is limited on a small scale.

Al_3Ti forms in $Al_{50}Ti_{50}$ powder after ball milling for 20 h with toluene as the PCA, as shown in Fig. 6. Ball milling makes Ti atoms dissolve into Al matrix as a result of interdiffusion reaction [20]. Ti in the Al matrix can form metastable Al_3Ti by solid−solid reaction because of the nearly equal formation enthalpy of TiH_2 (−144.3 kJ/mol) and Al_3Ti (−146.4 kJ/mol) [21].

The DSC test of ball-milled $Al_{50}Ti_{50}$ powder was performed to investigate the evolution process during heat treatment. Figure 8 shows the DSC curve of $Al_{50}Ti_{50}$ powder after ball milling for 20 h. There exists an exothermic peak induced by the decomposition of TiH_2 into Ti and H_2 in the temperature ranging from 675 to 823 K.

To testify the formation of the exothermic peak, the powder was heated to the corresponding peak temperature and then was cooled to room temperature rapidly. Subsequently, the heated powder was investigated by XRD, as shown in Fig. 9. The TiH_2 peak disappears after heating the ball-milled $Al_{50}Ti_{50}$ powder to 773 K, verifying the decomposition of TiH_2. While no Ti peak appears, which is supposed due to the alloying between Al matrix and Ti during heating process.

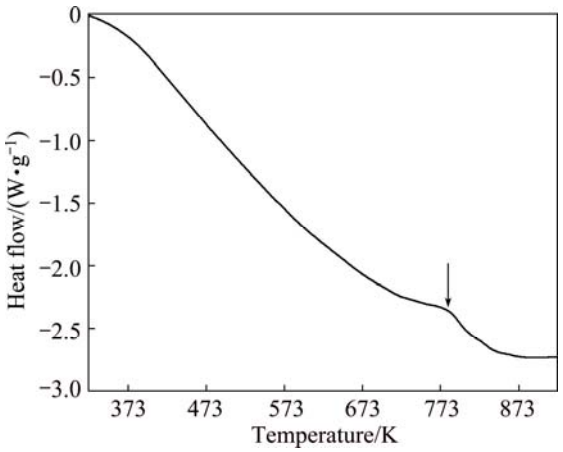

Fig. 8 DSC curve of $Al_{50}Ti_{50}$ powders after ball milling for 20 h

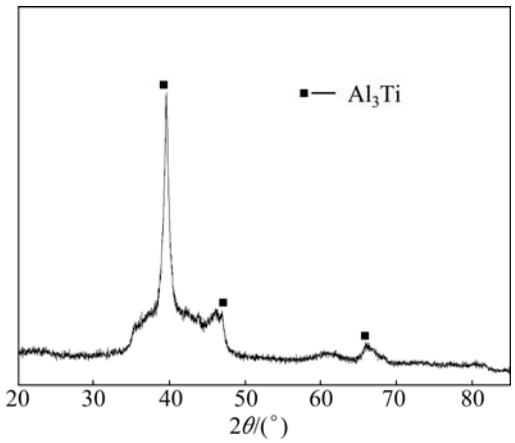

Fig. 9 XRD pattern of $Al_{50}Ti_{50}$ powders after finishing DSC test

5 Conclusions

1) The optimal amorphous $Al_{65}Cu_{16.5}Ti_{18.5}$ powder was obtained by combining the dual influences of fitting mole fractions of Cu and Ti elements and ball milling time. Increasing the mole fraction of Ti from 13.5% to 18.5% can promote the transformation from intermetallics to amorphous phase. Prolonging the ball milling time induces the dissolution of elements Al and Ti phases in $Al_{65}Cu_{16.5}Ti_{18.5}$ powder, thus reducing the crystalline phase to almost none, while the extension of ball milling time has nearly no influence on the $Al_{65}Cu_{35-x}Ti_x$ (x=13.5, 15.0, 16.5 and 17.5) alloy.

2) There still exists a little TiH_2 in $Al_{65}Cu_{16.5}Ti_{18.5}$ amorphous powder after balling milling for 30 h. The formation of TiH_2 results from the joint effects of the transformation of HCP−FCC Ti and the formation of H atoms decomposed from toluene. The volume fraction of TiH_2 in $Al_{65}Cu_{16.5}Ti_{18.5}$ amorphous powder is measured to be 4.30%. The DSC results demonstrate that TiH_2 is thermal metasable, TiH_2 is decomposed and Ti is re-alloyed with the matrix alloy after heating the powder to 675 K.

References

[1] WEI X, HAN F S, WANG X F, WANG X F, WEN C. Fabrication of Al-based bulk metallic glass by mechanical alloying and vacuum hot consolidation [J]. Journal of Alloys and Compounds, 2010, 501(1): 164−167.

[2] CAI A H, LIU Y, AN W K, ZHOU G J, LUO Y, LI T L, LI X S, TAN X F. Prediction of critical cooling rate for glass forming alloys by artificial neural network [J]. Materials Design, 2013, 52: 671−676.

[3] SAGEL A, WUNDERLICH R K, FECHT H J. Formation and crystallization behavior of amorphous $Zr_{60}Al_{10}Ni_9Cu_{18}Co_3$ produced by mechanical alloying and rapid quenching [J]. Materials Science Forum, 1997, 235−238: 389−394.

[4] ENAYATI M H, SCHUMACHER P. Amorphization of $Ni_{60}Nb_{20}Zr_{20}$ by mechanical alloying [J]. Materials Science and Engineering A, 2004, 375−377: 812−814.

[5] SCHLORKE N, ECKERT J, SCHULTZ L. Formation and stability of bulk metallic glass forming Mg−Y−Cu alloys produced by mechanical alloying and rapid quenching [J]. Materials Science Forum, 1998, 269−272: 761−766.

[6] KRASNOWSKI M, ANTOLAK-DUDKA A, KULIK T. Bulk amorphous $Al_{85}Fe_{15}$ alloy and $Al_{85}Fe_{15}$-B composites with amorphous or nanocrystalline-matrix produced by consolidation of mechanically alloyed powders [J]. Intermetallics, 2011, 19: 1243−1249.

[7] YUAN Yan-bo, WANG Zhi-wei, ZHENG Rui-xiao, HAO Xiao-ning, AMEYAMA Kei, MA Chao-li. Effect of mechanical alloying and sintering process on microstructure and mechanical properties of

Al−Ni−Y−Co−La alloy [J]. Transactions of Nonferrous Metals Society of China, 2014, 24(7): 2251−2257.
[8] MULA S, MONDAL K, GHOSH S, PABI S K. Structure and mechanical properties of Al−Ni−Ti amorphous powder consolidated by pressure-assisted and spark plasma sintering [J]. Materials Science and Engineering A, 2010, 527: 3757−3763.
[9] WANG W H, XIAO K Q, DONG Y D, HE Y Z, WANG M. A study on mechanically alloyed amorphous AlFe powder by X-ray diffraction and Mo¨ ssbauer spectroscopy [J]. Journal of Non-crystalline Solids, 1990, 124(1): 82−85.
[10] ZHANG Y F, LU L, YAP S M. Prediction of the amount of PCA for mechanical milling [J]. Journal of Materials Processing Technology 1999, 89−90: 260−265.
[11] KLEINER S, BERTOCCO F, KHALID F A, BEFFORT O. Decomposition of process control agent during mechanical milling and its influence on displacement reactions in the Al−TiO_2 system [J]. Materials Chemistry and Physics, 2005, 89: 362−366.
[12] JUÁREZ R, SUNOL J J, BERLANGA R, BONASTRE J, ESCODA L. The effects of process control agents on mechanical alloying behavior of a Fe−Zr based alloy [J]. Journal of Alloys and Compounds, 2007, 434−435: 472−476.
[13] AVAR B, OZCAN S. Structural evolutions in Ti and TiO_2 powders by ball milling and subsequent heat-treatments [J]. Ceramics International, 2014, 40: 11123−11130.
[14] JOHNSON W C, LEE J K, SHIFLET G J. Thermodynamic treatment of cyclic amorphization during ball milling [J]. Acta Materialia, 2006, 54(19): 5123−5133.
[15] SLUITER M, KAWAZOE Y. A simple model for the cyclic amorphization phenomenon [J]. Acta Materialia, 1999, 47(2): 475−480.
[16] MASSALSKI T B, OKAMOTO H. Binary alloys phase diagram [M]. 2nd ed. Ohio: ASM International, 1990.
[17] MANNA I, CHATTOPADHYAY P P, NANDI P, BANHART F, FECHT H J. Formation of face-centered-cubic titanium by mechanical attrition [J]. Journal of Applied Physics, 2003, 93: 1520−1524.
[18] PHASHA M J, BOLOKANG A S, NGOEPE P E. Solid-state transformation in nanocrystalline Ti induced by ball milling [J]. Materials Letters, 2010, 64(10): 1215−1218.
[19] WERT C H A. Trapping of hydrogen in metals [J]. Hydrogen in Metals II, 1978, 2: 305−330.
[20] LI Xue-wen, SUN Hong-fei, FANG Wen-bin, DING Yong-feng. Structure and morphology of Ti−Al composite powders treated by mechanical alloying [J]. Transactions of Nonferrous Metals Society of China, 2011, 21(S2): s338−s341.
[21] BARIN I. Thermochemical data of pure substances [M]. 3rd ed. Weinheim: VCH Ver-lagsgesllchaff mbH, 1989.

元素微调对机械合金化 Al−Cu−Ti 非晶合金成分优化的影响

谈 震[1]，薛云飞[1,2]，程兴旺[1,2]，张 龙[3]，陈为为[1,2]，王 鲁[1,2]，张海峰[3]，付华萌[3]

1. 北京理工大学 材料科学与工程学院，北京 100081；
2. 北京理工大学 冲击环境材料技术国家重点实验室，北京 100081；
3. 中国科学院金属研究所 沈阳材料科学国家实验室，沈阳 110016

摘 要：为了将 Al−Cu−Ti 非晶合金中的晶体相含量降到最低，通过调整 Cu 和 Ti 元素的含量和球磨时间对 $Al_{65}Cu_{35-x}Ti_x$ 合金进行优化设计。研究结果表明：增加 Ti 元素的含量能够降低 $AlCu_2Ti$、Cu_9Al_4 和 Al_2Cu 等金属间化合物的含量；而延长球磨时间可以降低合金中元素相的含量，最终确定的最优成分为 $Al_{65}Cu_{16.5}Ti_{18.5}$。另外，所有优化合金中都存在 TiH_2 相，这是由于在球磨作用下工程控制剂甲苯分解出的 H 原子与 Ti 元素反应生成了 TiH_2。TiH_2 在最优成分 $Al_{65}Cu_{16.5}Ti_{18.5}$ 合金中的体积分数为 4.30%。

关键词：Al 基非晶合金；工艺优化；湿混；TiH_2

(Edited by Mu-lan QIN)